Partitioning variance in cortical morphometry into genetic, environmental, and subject-specific components using a large adolescent sample

Authors: Diana M. Smith[1-4], Pravesh Parekh[5], Joseph Kennedy[3-4], Robert Loughnan[6], Oleksandr Frei[5,7], Thomas E. Nichols[8-9], Ole A. Andreassen[5], Terry L. Jernigan[3,10-12], Anders M. Dale[4,10-13]

Author Affiliations:

[1]Medical Scientist Training Program, University of California San Diego, La Jolla, CA.

[2]Neurosciences Graduate Program, University of California San Diego, La Jolla, CA.

[3]Center for Human Development, University of California, San Diego, La Jolla, CA.

[4]Center for Multimodal Imaging and Genetics, University of California, San Diego School of Medicine, La Jolla, CA.

[5]NORMENT, Division of Mental Health and Addiction, Oslo University Hospital & Institute of Clinical Medicine, University of Oslo, Oslo, Norway

[6]Population Neuroscience and Genetics Lab, University of California, San Diego, La Jolla, CA.

[7]Centre for Bioinformatics, Department of Informatics, University of Oslo, Oslo, Norway

[8]Big Data Institute, Li Ka Shing Centre for Health Information and Discovery, Nuffield Department of Population Health, University of Oxford, Oxford, UK

[9]Wellcome Centre for Integrative Neuroimaging, FMRIB, Nuffield Department of Clinical Neurosciences, University of Oxford, Oxford, UK

[10]Department of Cognitive Science, University of California, San Diego, La Jolla, CA.

[11]Department of Radiology, University of California, San Diego School of Medicine, La Jolla, CA.

[12]Department of Psychiatry, University of California, San Diego School of Medicine, La Jolla, CA.

[13]Department of Neuroscience, University of California, San Diego School of Medicine, La Jolla, CA.

Running head: Variance components of cortical phenotypes

Corresponding Author:
Diana M. Smith
9452 S Medical Ctr Dr
4th Floor, #4W217 C12
La Jolla, CA 92037
Tel: (617) 360-1280
d9smith@health.ucsd.edu

Abstract

The relative contributions of genetic variation and experience in shaping the morphology of the adolescent brain are not fully understood. Using longitudinal data from 11,665 subjects in the ABCD Study®, we fit vertex-wise variance components including family effects, genetic effects, and subject-level effects using a computationally efficient framework. Variance in cortical thickness and surface area is largely attributable to genetic influence, whereas sulcal depth is primarily explained by subject-level effects.

Main

The heritability of cortical brain imaging phenotypes has been a subject of investigation for several years. Prior studies have employed both twin datasets[1] and genome-wide association studies (GWAS)[2–4] to estimate the contribution of genetic variation to variance in cortical morphometry[5] at the region of interest (ROI) and vertex level.[6,7] Longitudinal datasets that capture changes in brain structure over time, such as the large Adolescent Brain Cognitive Development Study (ABCD Study®), can provide novel insights into the heritability of brain structure. However, due to study design, they demand the use of mixed-effects models that can account for family structure and repeated observations in addition to genetic relatedness. Until recently, vertex-wise mixed-effects models assessing the influence of shared genetic variance, as well as family- and subject-specific variance, on cortical morphometry have not yet been available, due in part to the computational demand of running complex models on tens of thousands of cortical vertices. Here we used a novel computational method to apply mixed-effects models to the large sample and the longitudinal design of the ABCD Study®, in order to estimate the contribution of genetic relatedness (heritability), shared family environment, and subject-specific variance to vertex-wise measures of brain morphometry.

To examine the spatial distributions of random effects across vertex-wise cortical measures, we applied a novel method, Fast and Efficient Mixed-Effects Algorithm (FEMA),[8] which can model genetic relatedness as a continuous value ranging from 0 to 1, rather than assigning categorical variables based on kinship. FEMA also allows for the flexible specification of several random effects simultaneously including shared family, subject ID, and others.[8] By using the full ABCD Study® sample (n=11,880) rather than restricting our analyses to twins, we were able to better approximate the variance components that exist in a general population. This approach to heritability analysis also has the potential to capture more shared variance than the heritability estimates obtained from GWAS, which only model the additive effects that can be inferred from common SNPs and therefore may not capture variance attributable to structural variants, rare variants, or non-additive effects.[9]

We estimated the contribution of additive genetic relatedness (akin to a heritability estimate), shared family environment (the extent to which siblings and twins share variance, coded as shared family ID), and the effect of subject (variance that is *not* explained by fixed effect covariates nor genetic/family structure, but nevertheless remains stable for a given subject over time). Of note, classical additive genetic / common environment / unique environment (ACE) models typically include data from a single timepoint and therefore cannot inspect the contribution of subject-specific variance in this manner. Using longitudinal neuroimaging data from the ABCD Study® release 4.0, we derived vertex-wise cortical thickness, cortical surface area, and sulcal depth. Then, for each vertex, we used the FEMA package[8] to fit the model

$$y \sim 1 + age + sex + scanner + software + A + C + S + E \quad (1)$$

where y represents the phenotype at each vertex; age, sex, MRI scanner, and scanner software version are fixed effect covariates; A, C, S, and E are the random effects, with their estimates corresponding to the proportion of variance in the phenotype (not explained by fixed effects) attributable to genetic similarity (A), common family environment (C, coded as family ID), subject (S), and the remaining unexplained variance (E), respectively.

Supplementary Figure 1 presents the total residual variance, ${\sigma^2}_{total}$, for cortical thickness, cortical surface area, and sulcal depth. The total residual variance ${\sigma^2}_{total}$ represents the phenotypic variance that is unexplained by the fixed effects included in our model; ${\sigma^2}_{total}$ is eventually partitioned into A, C, S, and E components. Figure 1 presents vertex-wise variance component estimates for cortical surface area as a

fraction of total residual variance, ${\sigma^2}_{total}$. The C component accounted for a small proportion of residual variance across the whole brain (Fig. 1). Supp. Fig. 2 displays the distribution of random effects estimates within each region of interest (ROI); C estimates ranged from 0.11 (supramarginal gyrus) to 0.26 (temporal pole; Supp. Fig. 2). The A component accounted for a larger proportion of variance, with visual inspection finding the strongest contributions in the medial frontal and occipital cortices, as well as the superior frontal gyrus (Fig. 1). When grouping vertices by ROI, mean A component estimates ranged from 0.28 (entorhinal cortex) to 0.57 (pericalcarine cortex; Supp. Fig. 2). Subject-specific variance S accounted for the largest proportion of variance in cortical surface area across several regions including the cingulate cortex and multiple regions of the parietal cortex. After grouping vertices into ROIs, the mean S estimates ranged from 0.19 (rostral anterior cingulate cortex) to 0.51 (inferior parietal cortex; Supp. Fig. 2).

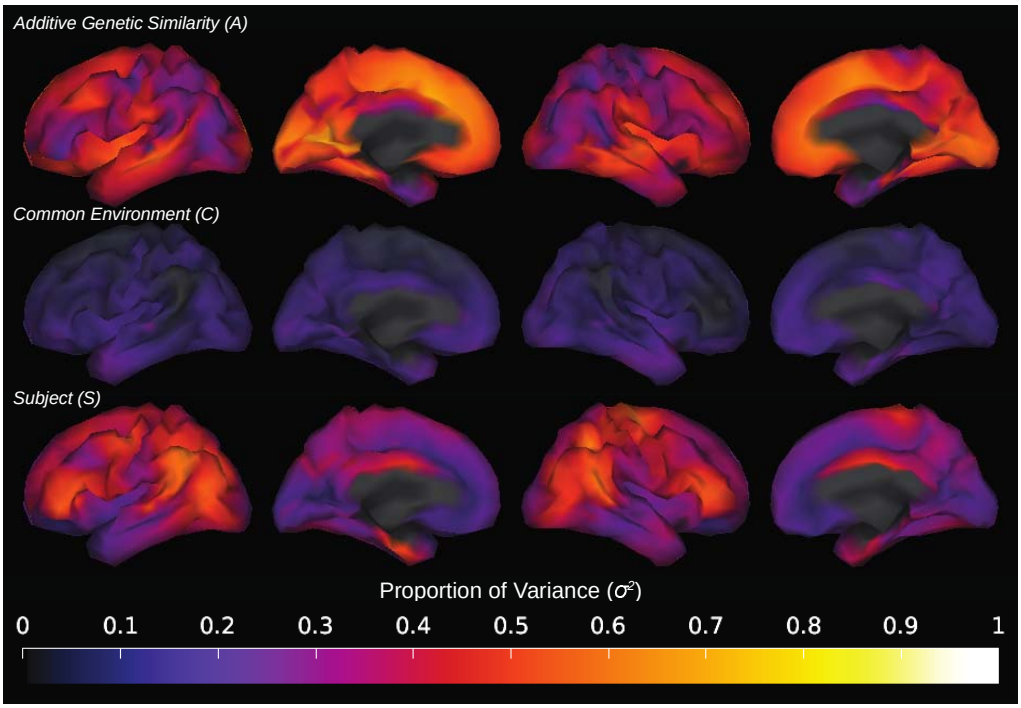

Figure 1. *Additive genetic (A), common environment (C), and subject-specific variance (S) components in cortical surface area, presented vertex-wise as a fraction of total residual variance.*

Figure 2 presents vertex-wise variance component results for cortical thickness; ROI-wise results are presented in Supp. Fig. 3. The A component accounted for a large proportion of residual variance, with particularly strong effects in the frontal and occipital cortices (Fig. 2). After grouping vertices into ROIs, the mean A component estimates across all vertices within an ROI ranged from 0.19 (temporal pole) to 0.44 (cuneus; Supp. Fig. 3). The S component also accounted for a substantial proportion of variance, particularly in the medial parietal and cingulate cortices, superior parietal lobule, and superior temporal gyrus (Fig. 2). After grouping vertex-level estimates into ROIs, mean S estimates across vertices within ROIs ranged from 0.25 (pericalcarine cortex) to 0.42 (isthmus of cingulate cortex; Supp. Fig. 3). Similar to cortical surface area, the C component accounted for relatively smaller proportions of residual variance across the cortex (Fig. 2); at ROI level, mean estimates for the C component ranged from 0.09 (pars opercularis) to 0.17 (lingual cortex; Supp. Fig. 3).

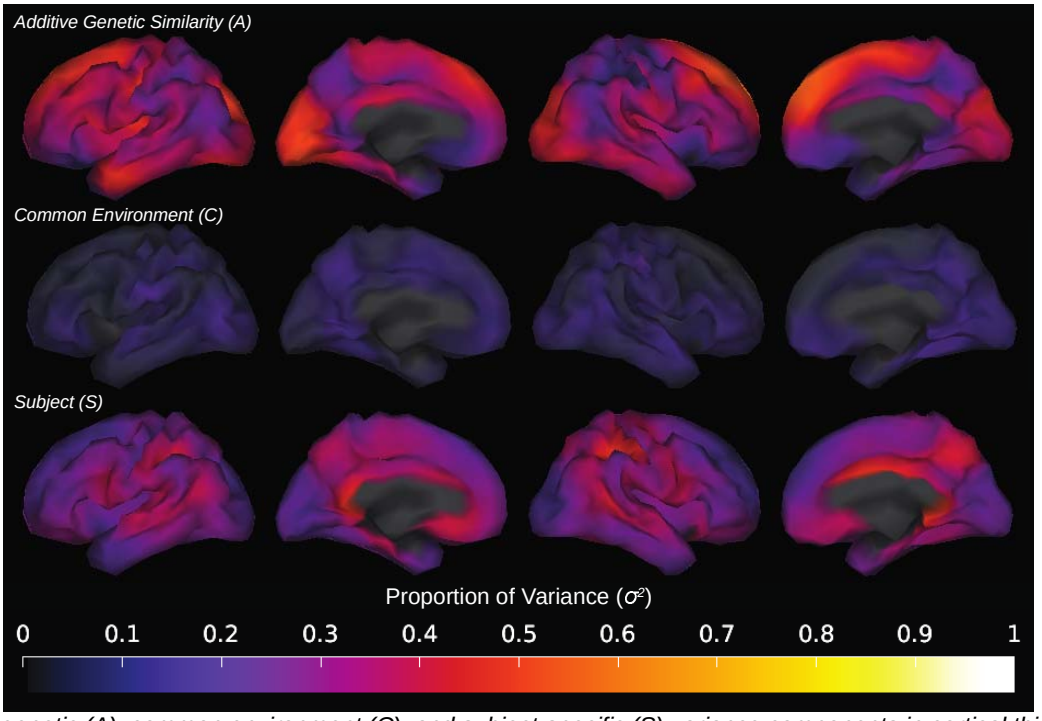

Figure 2. *Additive genetic (A), common environment (C), and subject-specific (S) variance components in cortical thickness, presented vertex-wise as a fraction of total residual variance.*

Figure 3 presents vertex-wise variance component estimates for sulcal depth. The C component accounted for a relatively small proportion of variance, and A accounted for a moderate proportion of variance. However, S accounted for a large proportion of variance across the entire cortex, with variance component estimates ranging from 0.34 (temporal pole) to 0.74 (caudal middle frontal gyrus; Supp. Fig. 4). Supplementary Figure 5 presents the A, C, and S variance components in a single summary figure using a red-green-blue color map for ease of interpretation.

Our analysis extends previous investigations of heritability based on twin data[6] and SNP-derived genetic relatedness data[2,3]. While twin heritability studies typically estimate variance components attributable to additive genetic relatedness and shared family, this analysis leverages the ABCD Study® longitudinal data to estimate an additional variance component that is attributable to subject-specific variance, i.e., the variance that is stable within a given participant over multiple study visits. This S component accounted for a large proportion of phenotypic variance in all cortical phenotypes studied, representing that this phenotype has a large proportion of variance that is *not* attributable to genetics, common family environment, or the fixed effects, but nevertheless remains stable in a given participant. In particular, the large contribution of the S component to sulcal depth, in combination with the relatively smaller estimates for A and C, indicates that this phenotype has a smaller genetic heritability and may represent a “fingerprint” phenotype that can differ between identical twins while remaining stable for a given participant over time.

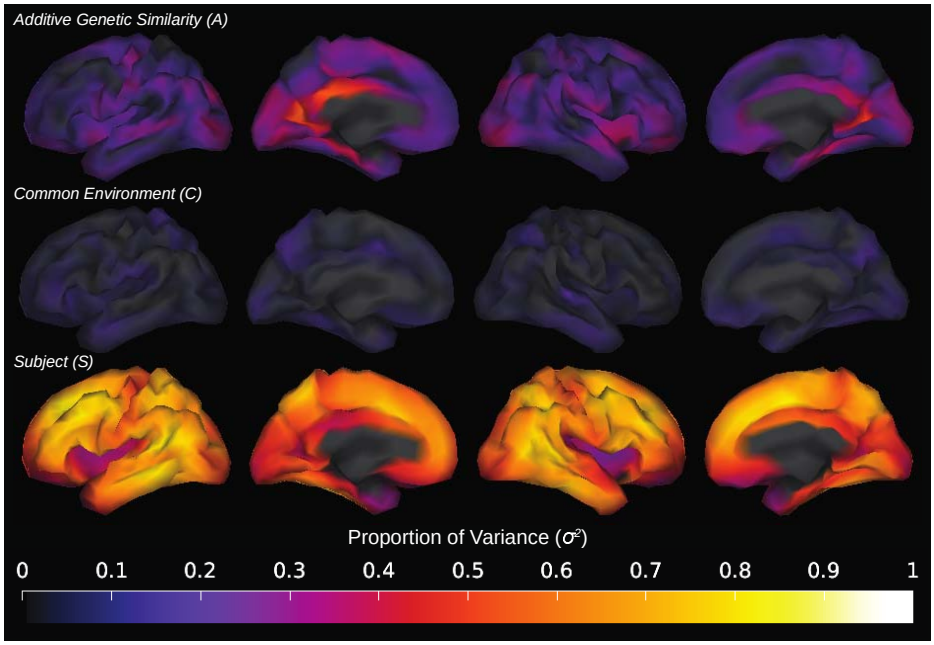

Figure 3. *Additive genetic (A), common environment (B), and subject-specific (C) variance components in sulcal depth, presented vertex-wise as a fraction of total residual variance.*

To our knowledge this analysis is the first to estimate vertex-wise heritability of cortical thickness and surface area in a large study of adolescents. Compared to a recent ROI-based study using the ABCD Study® twin sample[6], our A estimates were smaller, though larger than single nucleotide polymorphism (SNP) heritability estimates derived from GWAS[2,3]. This is consistent with prior comparisons of twin versus non-twin analyses in the ABCD Study®[10]. Notably, compared to classic twin studies, the present analysis incorporated the full ABCD Study® sample including siblings and unrelated participants, which may lead to narrower confidence intervals when estimating heritability[10]. Consistent with previous findings that vertex-wise heritability estimates can differ from ROI-based estimates[7], the present study provides evidence that genetic contributions to cortical structure can vary continuously even within a region of the cortex. In addition, the vertex-level distribution of random effects within ROIs confirms that traditional anatomical parcellations do not necessarily match genetic parcellations[1,11]. The present study confirms and extends prior literature estimating heritability of cortical phenotypes in adolescents[6], using a novel statistical package to leverage the full ABCD Study® sample across multiple timepoints. While the mixed-effects models used in this work remain agnostic regarding the specific sources of genetic influence, future work should aim to incorporate genomic data to better understand the specific longitudinal contributions of genetic variation to adolescent brain development.

Methods

Sample

The ABCD Study® is an ongoing longitudinal multisite study within the United States that includes data from 11,880 adolescents recruited from 21 data acquisition sites[12,13]. Each site obtained approval from their Institutional Review Board, and all participants and caregivers underwent verbal and written consent/assent. Exclusion criteria for the ABCD Study® include 1) lack of English proficiency in the child; 2) the presence of severe sensory, neurological, medical or intellectual limitations that would inhibit the child's ability to comply with the study protocol; 3) an inability to complete an MRI scan at baseline. In this study, we used baseline and the first follow-up imaging data (acquired two years after the baseline) from ABCD release 4.0. We included all individuals with imaging and genomics data that passed quality control; analyses were restricted to observations with complete imaging and covariate data (final N = 11,402 at baseline, 7,695 at 2 year follow-up, for a total of 19,097 observations; mean age at first visit = 9.92 years (SD = 0.62), % female at first visit: 48.0). Supplementary Table 1 shows the demographics of the analytic sample at baseline and at the follow up.

Genotyping, Genetic Principal Components and Genetic Relatedness

Methods for collecting genetic data have been described in detail elsewhere[14]. Briefly, a saliva sample was collected at the baseline visit, as well as a blood sample from twin pairs. The Smokescreen™ Genotyping array[15] was used to assay over 500,000 single nucleotide polymorphisms (SNPs), which were used for genetic

relatedness calculation using PC-Air[16] and PC-Relate[17]. PC-AiR captures ancestry information that is not confounded by relatedness by finding a set of unrelated individuals in the sample that have the highest divergent ancestry and computes the PCs in this set; the remaining related individuals are then projected into this space. PC-Relate computes a GRM that is Independent from ancestry effects as derived from PC-AiR. PC-AiR was run using the default suggested parameters from the GENESIS package[18], as described in previous work[10]. Supplementary Figure 6 displays a histogram of the pairwise genetic relatedness values across the full sample (Supp. Fig. 6A) as well as the subset of pairs of participants with shared family ID (Supp Fig. 6B). Of the 2011 pairs of individuals that shared a family ID, 1868 pairs had genomic relatedness data; of these, 1378 pairs had genetic relatedness between 0.25 and 0.75 (most likely full siblings or dizygotic twins) and 389 pairs had genetic relatedness greater than 0.75 (most likely monozygotic twins).

MRI acquisition and image processing

The ABCD Study® MRI data were collected across 21 research sites using Siemens Prisma, GE 750 and Philips Achieva and Ingenia 3 T scanners. Scanning protocols were harmonized across sites. Details of imaging acquisition and processing protocols used in the ABCD Study® have been described previously[19,20]. Briefly, T1-weighted images were acquired using a 3D magnetization-prepared rapid acquisition gradient echo (MPRAGE) scan with 1 mm isotropic resolution and no multiband acceleration. T1w structural images were corrected for gradient nonlinearity distortions using scanner-specific, nonlinear transformations provided by MRI scanner manufacturers[21,22]. Intensity inhomogeneity correction was performed by applying smoothly varying, estimated B1-bias field[20]. Images were rigidly registered using a cross-sectional framework and resampled into alignment with a pre-existing, in-house, averaged, reference brain with 1.0 mm isotropic resolution[20]. Cortical surface reconstruction was conducted using FreeSurfer v7.1.1, which includes tools for estimation of various measures of brain morphometry and uses routinely acquired T_1w MRI volumes[23–32]. The cortical parcellation used in this analysis was conducted in FreeSurfer using the Desikan-Kiliany cortical atlas[33]. All analyses included only those participants who were recommended for inclusion in post-processed sMRI quality control (imgincl_t1w_include==1).

Statistical analysis

The classic ACE model used to estimate heritability is equivalent to a linear mixed-effects (LME) model specified as follows:

$$y_i = \mu + x'_i\beta + A_i + C_i + E_i \qquad (2)$$

where y_i is the trait value of the ith scan; μ is the overall mean; x_i denotes a vector of covariates; and A_i , C_i , E_i represent latent additive genetic, common family and unique environmental random effects, respectively. Over subjects, the covariance of these three terms are $\sigma_A^2\Sigma_A$, $\sigma_C^2\Sigma_C$, and $\sigma_E^2 I$; Σ_A is given by the genetic relatedness, which could be a kinship coefficient (e.g. ½ for siblings or dizygotic twins) or, as we have done, the SNP-wise genetic similarity similar to previous methods[34]; Σ_C has 1's on off-diagonals for any family pairs, 0 otherwise.

For longitudinal datasets incorporating data from multiple timepoints for a given participant, an additional random effect S can be incorporated:

$$y_i = \mu + x'_i\beta + A_i + C_i + S_i + E_i \qquad (3)$$

where S_i is the random effect of subject (e.g., subject ID), and the vector of covariates x_i includes a fixed effect to incorporate multiple timepoints (e.g., age). The covariance of the subject effect is $\sigma_S^2\Sigma_S$, where Σ_S has 1's on off diagonals observation pairs from the same subject; with a subject effect modeled, the final effect E_i corresponds to a pure intrasubject measurement error. Note that the total residual variance, $\sigma_{total}^2 = \sigma_A^2 + \sigma_C^2 + \sigma_S^2 + \sigma_E^2$, is the same variance that would be estimated in a cross-sectional analysis of unrelated subjects, and demonstrates how this approach decomposes all phenotypic variance into meaningful components.

Vertex-wise analysis

Univariate linear mixed effects models (LMMs) were applied at each vertex to model cortical morphometry (cortical thickness, cortical surface area, sulcal depth) as the dependent variables.

All of the results shown are from a model including age, sex, MRI scanner and software version as fixed covariates. Random effects were modeled as genetic relatedness (A) and subject (S) nested within shared family groups (C). All LMMs were run using the publicly available FEMA software package[8], which handles voxel- and vertex-wise data and can incorporate a matrix of SNP-derived genetic relatedness.

For the main results, vertex-wise statistical maps present σ^2, the proportion of residual variance that is explained by variance in the random effect of interest. Unthresholded σ^2 maps are presented in the main figures to provide a comprehensive description of the continuous distribution of effects. Supplementary Figure 1 displays the total residual variance, σ^2_{total}, which is the total unexplained variance after accounting for the fixed effects in the model (age, sex, scanner, and software). σ^2_{total} is displayed in units that match the units of the phenotype of interest (mm or mm^2) and represents the total phenotypic variance that is then partitioned into *A*, *C*, *S*, and *E* components. For the summary figure displayed in Supplementary Figure 5, red-green-blue color values were determined by assigning a red value based on the additive genetic component, green based on the common environment component, and blue based on the subject specific variance component.

Region-of-interest (ROI) analyses

To visualize the distribution of test statistics by region of interest (ROI), the vertex-level test statistics were mapped to the corresponding regions of interest (ROIs) in the Desikan-Kiliany 40 Atlas[33]. Violin plots were generated to show the distribution of vertex-level effects across all vertices within each ROI mask, stratified by hemisphere, to highlight the range of effects within each ROI.

All statistical analyses were conducted using custom code in MATLAB v2020a. FEMA is publicly available on GitHub (https://github.com/cmig-research-group/cmig_tools).

Data availability

ABCD Study® data release 4.0 is available for approved researchers in NIMH Data Archive (NDA; http://dx.doi.org/10.15154/1523041).

Code availability

The code to analyze the data and generate all figures of this manuscript is available on GitHub: https://github.com/dmysmith/random_effects

Acknowledgements and Conflicts of Interest

Data used in the preparation of this article were obtained from the Adolescent Brain Cognitive Development℠ (ABCD) Study (https://abcdstudy.org), held in the NIMH Data Archive (NDA). This is a multisite, longitudinal study designed to recruit more than 10,000 children age 9-10 and follow them over 10 years into early adulthood. The ABCD Study® is supported by the National Institutes of Health and additional federal partners under award numbers U01DA041048, U01DA050989, U01DA051016, U01DA041022, U01DA051018, U01DA051037, U01DA050987, U01DA041174, U01DA041106, U01DA041117, U01DA041028, U01DA041134, U01DA050988, U01DA051039, U01DA041156, U01DA041025, U01DA041120, U01DA051038, U01DA041148, U01DA041093, U01DA041089, U24DA041123, U24DA041147. A full list of supporters is available at https://abcdstudy.org/federal-partners.html. A listing of participating sites and a complete listing of the study investigators can be found at https://abcdstudy.org/consortium_members/. ABCD consortium investigators designed and implemented the study and/or provided data but did not necessarily participate in the analysis or writing of this report. This manuscript reflects the views of the authors and may not reflect the opinions or views of the NIH or ABCD consortium investigators.

The ABCD data repository grows and changes over time. The ABCD data used in this report came from ABCD Study Data Release 4.0 (http://dx.doi.org/10.15154/1523041). DOIs can be found at https://nda.nih.gov/abcd/abcd-annual-releases.html.

The authors wish to thank the youth and families participating in the ABCD Study® and all staff involved in data collection and curation. The work was also funded by the European Union's Horizon 2020 research and innovation programme (grant agreement number *964874* to Dr Andreassen, Marie Skłodowska-Curie grant

agreement number 801133 to Dr Parekh) and from the Research Council of Norway (#223273, # 324252, *#324499)*. D. Smith was supported by Kavli Innovative Research Grant under award number 2022-2195 for this project. Dr. Dale reports that he was a Founder of and holds equity in CorTechs Labs, Inc., and serves on its Scientific Advisory Board. He is a member of the Scientific Advisory Board of Human Longevity, Inc. He receives funding through research grants from GE Healthcare to UCSD. The terms of these arrangements have been reviewed by and approved by UCSD in accordance with its conflict of interest policies. Dr. Andreassen has received speaker fees from Janssen, Lundbeck and Sunovion and is a consultant to Cortechs.ai. The remaining authors have no conflicts of interest.

References

1. Chen, C.-H. *et al.* Genetic topography of brain morphology. *Proc. Natl. Acad. Sci.* **110**, 17089–17094 (2013).
2. Shadrin, A. A. *et al.* Vertex-wise multivariate genome-wide association study identifies 780 unique genetic loci associated with cortical morphology. *NeuroImage* **244**, 118603 (2021).
3. van der Meer, D. *et al.* The genetic architecture of human cortical folding. *Sci. Adv.* **7**, eabj9446 (2021).
4. Yang, J., Zeng, J., Goddard, M. E., Wray, N. R. & Visscher, P. M. Concepts, estimation and interpretation of SNP-based heritability. *Nat. Genet.* **49**, 1304–1310 (2017).
5. Chen, C.-H. *et al.* Large-scale genomics unveil polygenic architecture of human cortical surface area. *Nat. Commun.* **6**, 7549 (2015).
6. Maes, H. H. M. *et al.* Genetic and environmental variation in continuous phenotypes in the ABCD Study®. *Behav. Genet.* **53**, 1–24 (2023).
7. Eyler, L. T. *et al.* A Comparison of Heritability Maps of Cortical Surface Area and Thickness and the Influence of Adjustment for Whole Brain Measures: A Magnetic Resonance Imaging Twin Study. *Twin Res. Hum. Genet.* **15**, 304–314 (2012).
8. Parekh, P. *et al.* FEMA: Fast and efficient mixed-effects algorithm for large sample whole-brain imaging data. 2021.10.27.466202 Preprint at https://doi.org/10.1101/2021.10.27.466202 (2023).
9. Génin, E. Missing heritability of complex diseases: Case solved? *Hum. Genet.* **139**, 103–113 (2020).
10. Smith, D. M. *et al.* Heritability Estimation of Cognitive Phenotypes in the ABCD Study® Using Mixed Models. *Behav. Genet.* **53**, 169–188 (2023).
11. Chen, C.-H. *et al.* Hierarchical Genetic Organization of Human Cortical Surface Area. *Science* **335**, 1634–1636 (2012).
12. Garavan, H. *et al.* Recruiting the ABCD sample: Design considerations and procedures. *Dev. Cogn. Neurosci.* **32**, 16–22 (2018).
13. Volkow, N. D. *et al.* The conception of the ABCD study: From substance use to a broad NIH collaboration. *Dev. Cogn. Neurosci.* **32**, 4–7 (2018).
14. Uban, K. A. *et al.* Biospecimens and the ABCD study: Rationale, methods of collection, measurement and early data. *Dev. Cogn. Neurosci.* **32**, 97–106 (2018).
15. Baurley, J. W., Edlund, C. K., Pardamean, C. I., Conti, D. V. & Bergen, A. W. Smokescreen: a targeted genotyping array for addiction research. *BMC Genomics* **17**, 145 (2016).
16. Conomos, M. P., Miller, M. B. & Thornton, T. A. Robust inference of population structure for ancestry prediction and correction of stratification in the presence of relatedness. *Genet. Epidemiol.* **39**, 276–293 (2015).
17. Conomos, M. P., Reiner, A. P., Weir, B. S. & Thornton, T. A. Model-free estimation of recent genetic relatedness. *Am. J. Hum. Genet.* **98**, 127–148 (2016).
18. Gogarten, S. M. *et al.* Genetic association testing using the GENESIS R/Bioconductor package. *Bioinformatics* **35**, 5346–5348 (2019).
19. Casey, B. J. *et al.* The Adolescent Brain Cognitive Development (ABCD) study: Imaging acquisition across 21 sites. *Dev. Cogn. Neurosci.* **32**, 43–54 (2018).
20. Hagler, D. J. *et al.* Image processing and analysis methods for the Adolescent Brain Cognitive Development Study. *NeuroImage* **202**, 116091 (2019).
21. Jovicich, J. *et al.* Reliability in multi-site structural MRI studies: Effects of gradient non-linearity correction on phantom and human data. *NeuroImage* **30**, 436–443 (2006).
22. Wald, L., Schmitt, F. & Dale, A. Systematic spatial distortion in MRI due to gradient non-linearities. *NeuroImage* **6**, 50 (2001).
23. Dale, A. M., Fischl, B. & Sereno, M. I. Cortical Surface-Based Analysis: I. Segmentation and Surface Reconstruction. *NeuroImage* **9**, 179–194 (1999).
24. Fischl, B., Sereno, M. I. & Dale, A. M. Cortical Surface-Based Analysis: II: Inflation, Flattening, and a Surface-Based Coordinate System. *NeuroImage* **9**, 195–207 (1999).
25. Fischl, B., Sereno, M. I., Tootell, R. B. & Dale, A. M. High-resolution intersubject averaging and a coordinate system for the cortical surface. *Hum. Brain Mapp.* **8**, 272–284 (1999).
26. Dale, A. M. & Sereno, M. I. Improved Localizadon of Cortical Activity by Combining EEG and MEG with MRI Cortical Surface Reconstruction: A Linear Approach. *J. Cogn. Neurosci.* **5**, 162–176 (1993).
27. Fischl, B. & Dale, A. M. Measuring the thickness of the human cerebral cortex from magnetic resonance images. *Proc. Natl. Acad. Sci.* **97**, 11050–11055 (2000).

28. Fischl, B., Liu, A. & Dale, A. M. Automated manifold surgery: constructing geometrically accurate and topologically correct models of the human cerebral cortex. *IEEE Trans. Med. Imaging* **20**, 70–80 (2001).
29. Fischl, B. *et al.* Whole Brain Segmentation: Automated Labeling of Neuroanatomical Structures in the Human Brain. *Neuron* **33**, 341–355 (2002).
30. Fischl, B. *et al.* Automatically parcellating the human cerebral cortex. *Cereb. Cortex* **14**, 11–22 (2004).
31. Ségonne, F. *et al.* A hybrid approach to the skull stripping problem in MRI. *NeuroImage* **22**, 1060–1075 (2004).
32. Ségonne, F., Pacheco, J. & Fischl, B. Geometrically accurate topology-correction of cortical surfaces using nonseparating loops. *IEEE Trans. Med. Imaging* **26**, 518–529 (2007).
33. Desikan, R. S. *et al.* An automated labeling system for subdividing the human cerebral cortex on MRI scans into gyral based regions of interest. *NeuroImage* **31**, 968–980 (2006).
34. Yang, J., Lee, S. H., Goddard, M. E. & Visscher, P. M. GCTA: A tool for Genome-wide Complex Trait Analysis. *Am. J. Hum. Genet.* **88**, 76–82 (2011).